PROCEEDINGS OF THE INTERNATIONAL CONFERENCE
NANOMATERIALS: APPLICATIONS AND PROPERTIES
Vol. **2** No 2, 02PCN15(4pp) (2013)

Mechanochemical, Sonochemical and Hydrothermal Activation of Niobium Pentoxide and its Catalytic Properties

S. Khalameida[1,*], V. Sydorchuk[1], J. Skubiszewska-Ziéba[2], R. Leboda[2], V. Zazhigalov[1]

[1] *Institute of Sorption and Problems of Endoecology National Academy of Science of Ukraine, 13, Naumov Str., 03164, Kyiv, Ukraine*
[2] *Faculty of Chemistry, Maria Curie-Sklodowska, 3, pl. Marie Curie-Sklodowska, 20031, Lublin, Poland*

(Received 28 May 2013; published online 31 August 2013)

Modification of niobium pentoxide with different dispersity via mechanochemical, ultrasound, hydrothermal and microwave treatments (MChT, UST, HTT, and MWT, respectively) has been studied. All types of treatment do not change of phase composition but leads to improvement (at HTT and MWT) or, on contrary, breaking of crystal structure (at MChT and UST) and variation of crystallite size and specific surface area. UV-Vis measurements display increase of absorption in visible region. As a result, modified samples show higher photocatalytic activity at degradation of rhodamine B under visible irradiation. Similarly, initial and modified Nb_2O_5 samples are catalysts for mechanochtmical and sonochemical destruction of the same dye.

Keywords: Nb_2O_5, Mechanochemical, Sonochemichal, Hydrothermal activation**,** Rhomanin B destruction.

PACS number: 42.70.Qs

1. INTRODUCTION

Niobium pentoxide Nb_2O_5 as typical semiconductor with a high band gap [1] has attracted great research interest due to its remarkable applications in gas sensors, optical devices, and Li-ion batteries [2]. Besides, it is used as oxide, acid and photocatalyst [2, 3]. Therefore, Nb_2O_5 is versatile material. The influence of synthesis conditions on its physical-chemical characteristics is well studied. The application of non-conventional techniques for regulation properties of commercial niobium pentoxide powders is the aim of this work.

2. EXPERIMENTAL

2.1 Activation of Niobium Pentoxide

Sintered ceramic and three powders with different specific surface area S (dispersity) and phase composition were subjected to various types of modification: mechanochemical, hydrothermal, microwave and ultrasound treatments (MChT, HTT, MWT and UST, respectively). MChT (milling) was carried out in Pulverisette 6 planetary ball mill (Fritsch Gmbh) in air, ethanol and water at rotation speed of 300-850 rpm. HTT was performed using steel autoclaves with volume of 45 ml at 200 °C and the autogeneous pressure for 5 h. "NANO 2000" high-pressure reactor (Plazmatronika, Poland) with power of 650 W was used for MWT. In the latter case, treatment temperature and pressure were 200 °C and 4.5 MPa. UST was carried out in open reactor using UZDN ultrasonic disperser (Selmi, Ukraine) under frequency 20 KHz and 80 °C for 1.

2.2 Physical-chemical Characterizations

The starting reagents and products of their transformations were studied by means of X-ray powder diffraction (XRD) using Philips PW 1830 diffractometer with CuK_α-radiation. The primary crystallites size D_{hkl} was calculated using the broadening of the most intensive lines according to Sherrer's equation. Diffuse reflectance UV-Vis spectra of powders were registered on Lambda 35 UV-Vis spectrometer (Labsphere RSA-PE-20 diffuse reflectance and transmittance accessory, Perkin-Elmer Instruments). $BaSO_4$ was used as a reference. All spectra are presented in coordinates of Kubelka-Munk equation. Parameters of porous structure (specific surface area S, mesopores volume V_{me}) were determined from isotherms of nitrogen adsorption-desorption obtained with the help of ASAP 2405N analyzer ("Micromeritics Instrument Corp"). Outgassing temperature and duration before taking of measurements were 150 °C and 2 h, respectively.

2.3 Photocatalytic Activity

The testing of photocatalytic activity was carried out using degradation of textile dye rhodamine B (Rh B) in aqueous medium ($0.5 \cdot 10^{-5}$ mol L^{-1} solution). This reaction was performed in glass reactor with magnetic stirrer. The illumination was realized using high-intensity discharge Na lamp GE Lucalox (Hungary) with power 70 W which irradiates solely in visible region. The ratio catalyst / dye solution was 100 mg / 150 ml. The initial solution and that after dye degradation was analyzed spectrophotometrically at λ_{max} = 555 nm (Lambda 35, PerkinElmer Instruments) after centrifugation of reaction mixture (10 min at 8000 rpm). The calculation of photodegradation rate constants K_d was based on the concentration change of the solution after establishment of adsorption / desorption equilibrium.

3. RESULTS AND DISCUSSION

3.1. Modification of Low-dispersed Nb_2O_5

Diffractograms of initial and modified Nb_2O_5 with $S = 2$ $m^2 \cdot g^{-1}$ which is orthorhombic phase (JCPDS N 30-873) are depicted on Fig. 1. One can see that its phase composition does not changed as a result of

MChT during 1 h in different media (ethanol, water, air) and UST in water. However, intensity of reflexes I_{hkl} decreases and their width, on contrary, increases.

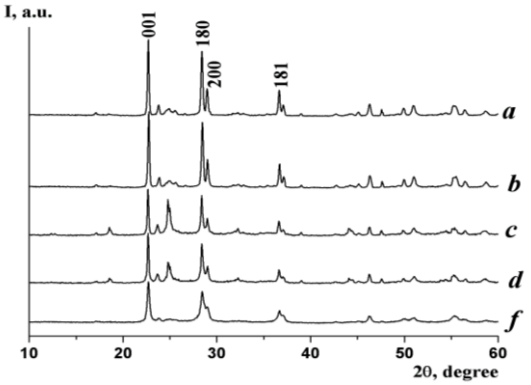

Fig. 1 – XRD patterns for low-dispersed Nb_2O_5: initial (a), after UST 1 h (b), MChT at 600 rpm 1 h in ethanol (c), water (d) and air (f)

Thus, I_{001} ($2\Theta = 22.72^o$) reduces in 1.5-1.8 times (maximum after dry milling). Crystallites size D_{001} also decreases: from 28.7 to 19.8-24.3 nm (Table, column 7). At the same time, UST of this sample for 1 h does not cause any changes in crystal structure (Fig. 1, curve *b*) which can be explained by small intensity of UST. UV-Vis spectra for samples milled on air also do not show considerable alteration in structure: main band is centered about 310-325 nm and absorption edge λ – at 380-380 nm (band gap $E_g \sim 3.25$ eV) which is agreed with literature data [4]. Samples prepared via MChT in water reveal certain bathochromic shift of λ to 393 nm which corresponds to values of $E_g = 3.15$ eV as in [5], for example.

The particles of low-dispersed Nb_2O_5 powder are practically non-porous which can be seen from calculations based on adsorption data. MChT and UST (first of all, short-time) promote increasing in specific surface area. At MChT, it is obviously caused by deaggregation of polycrystalline particles and breaking of primary crystallite. The latter is confirmed by calculations based on XRD data indicated above. Only first process takes place during UST since D_{001} value does not changed. Besides, pore volume increases as result of all types of modification which is associated with formation of phase contact between crystallites.

3.2. Modification of high-dispersed Nb_2O_5

High-dispersed Nb_2O_5 ($S = 355$ m$^2 \cdot$g^{-1}) is X-ray amorphous. Their modification results in improvement of crystal structure, namely, formation of orthorhombic phase (Fig. 2). It takes place under severe hydrothermal conditions: milling in water at 850 rpm or MWT at 200 ºC. Value of D_{001} equals 23.5 and 22.7 nm, respectively.

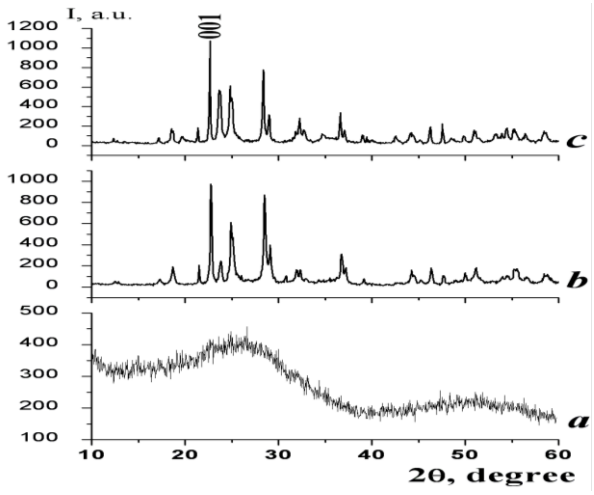

Fig. 2 – XRD patterns for high-dispersed Nb_2O_5: initial (a), after MChT at 850 rpm in water (b), MWT at 200 °C in water (c)

As can be seen on Fig. 3, UV-Vis spectrum for high-dispersed sample contain band at 275 nm while that for low-dispersed – at 319 nm (Fig. 3). This discrepancy can be explained by different dispersity and crystal structure of both Nb_2O_5. UST of high-dispersed samples also leads hypsochromic shift of absorption edge i.e.

Table 1 – Porous structure parameters of Nb_2O_5

N	Treatment conditions	S, m$^2 \cdot$g^{-1}	Vs, cm$^3 \cdot$g^{-1}	V_Σ, cm$^3 \cdot$g^{-1}	V_{me}, cm$^3 \cdot$g^{-1}	D_s, nm	D_{001}, nm
1	2	3	4	5	6	7	8
1	Initial low-dispersed	2.0	0.005	–	0.005	650	28.7
2	MChT air 300 rpm	2.8	0.01	–	0.01	470	24.3
3	MChT air 600 rpm	4.9	0.01	0.11	0.01	270	22.4
4	MChT water 600 rpm	6.0	0.02	0.15	0.02	220	19.8
5	MChT ethanol 600 rpm	3.0	0.01	0.05	0.01	445	21.9
6	UST 0.5 h	4.4	0.04	0.10	0.04	300	28.0
7	UST 1 h	2.8	0.03	0.06	0.03	470	29.2
8	HTT 200 ºC	1.8	0.02	0.02	0.02	725	32.3
9	Initial high-dispersed	355	0.29	0.30	0.12	4.0	–
10	MChT air 600 rpm	46	0.02	0.05	0.02	31	–
11	MChT air 850 rpm	14	0.06	0.07	0.06	100	–
12	MChT water 850 rpm	8.0	0.02	0.80	0.02	175	22.4
13	MWT 200 °C	55	0.07	0.48	0.07	24	25.1
14	UST 0.5 h	321	0.30	0.31	0.14	4.5	–
15	UST 1 h	333	0.32	0.32	0.17	4.5	–
16	HTT 200 °C	144	0.39	0.41	0.36	9.0	10.3

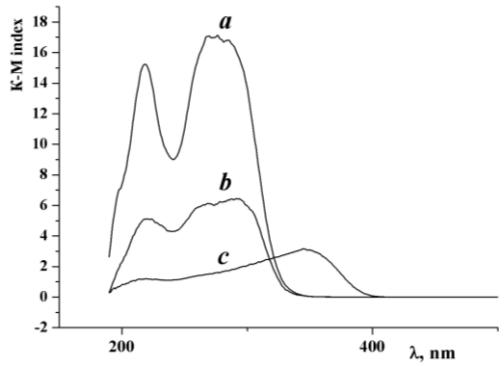

Fig. 3 – UV-Vis spectrum for high-dispersed Nb_2O_5: amorphous phase (a), the same after UST 1 h (b), orthorhombic phase after UST 1 h (c)

narrowing of band gap. Although high-dispersed sample is powder (free-dispersed state), its particles, are micro-mesoporous (Table). Modification of this sample, using all kinds of treatment, causes reduction of specific surface area which is maximal as a result of MChT and MWT. Modification in water promotes formation of porous framework through consolidation of particles. There is secondary porosity represented by macropores (total pore volume V_Σ > sorption pore volume V_s), as a result. Thus, value of macropores volume equals 0.32 $cm^3 \cdot g^{-1}$ or 80 % of total pore volume V_Σ for sample modified via MWT.

3.3. Photocatalytic Activity

Nb_2O_5 samples subjected to MChT and UST show higher absorption of visible light which is main reason of their photocatalytic activity (rate constant of Rh B degradation K_d) in this region. Clear relationship has been established: the values of specific surface area S and absorption in visible range is higher, the K_d magnitude is more.

For example, kinetic curves of Rh B degradation under visible irradiation in the presence of different modified samples are depicted on Fig. 4. Noteworthy that niobium pentoxide contributes to the rapid (during 10 min) deethylation of rhodamine *B* to rhodamine 110 (shift of band 555 towards 498-500 nm) and following decrease of intensity of this band (Fig. 5).

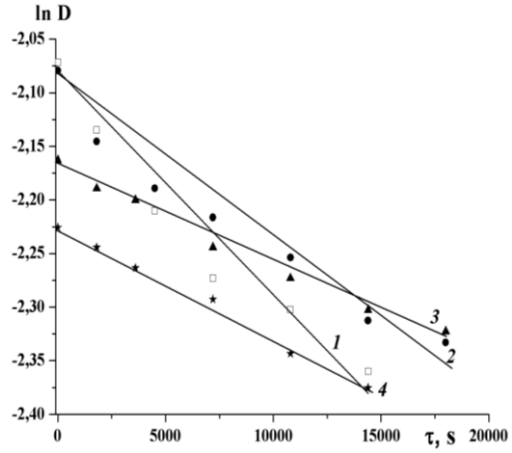

Fig. 4 – Kinetic curves for low-dispersed Nb_2O_5 after MChT in air at 300 rpm (1), 600 rpm (2), HTT at 200 °C (3), UST 1 h (4)

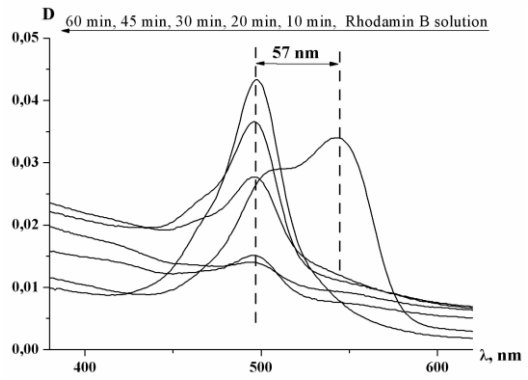

Fig. 5 – UV-Vis spectral changes of Rhodamin B aqueous solution in the presence of high-dispersed Nb_2O_5 after visible irradiation

The latter indicated destruction of chromophore ring in dye molecule. Value of K_d for this process, calculated using intensity of band 500 nm, equals $3.28 \cdot 10^{-4}$ and $4.22 \cdot 10^{-4}$ s^{-1} under UV- and visible irradiation, respectively. It is known that using of TiO_2 photocatalyst leads to slower stepwise diethylation of Rh B [6].

Five samples of Nb_2O_5 (with $S = 0.1$, 2, 3, 355 and 474 $m^2 \cdot g^{-1}$) were studied for mechanocatalytic degradation of RhB in aqueous solutions. It has been established the same antibate dependence between values of K_d and S for initial catalyst as for the titania samples [7]. The obtained relationship can be satisfactorily approximated by two nearly straight segments that are intersected, i.e. broken line (Fig. 6).

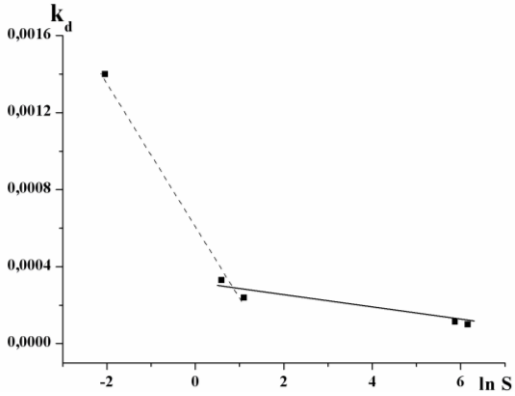

Fig. 6 – Dependence between the values of the rate constant of degradation and specific surface area of the catalyst

Therefore, K_d magnitude is maximal for the most low-dispersed sample ($1.4 \cdot 10^{-3}$ s^{-1}). On the contrary, value of K_d steadily increases within $1.1 \cdot 10^{-4}$-$1.1 \cdot 10^{-3}$ s^{-1} when specific surface area of Nb_2O_5 catalyst rises from 2 to 355 $m^2 \cdot g^{-1}$ under ultrasound degradation of Rh B.

4. CONCLUSION

Modification of low-dispersed Nb_2O_5 via mechanochemical and sonochemical treatments causes partial destruction of its crystal structure and increase of dispersity (specific surface area). Porous network is formed in aqueous medium. On contrary, crystal structure of high-dispersed Nb_2O_5 is improved as results of all types of modification. All modified sam-

ples show higher absorption of visible light. Increase of photo-, mechano-, and sonocatalytic activity of modified Nb_2O_5 in process of rhodamine B degradation takes place.

AKNOWLEDGEMENTS.

This work was supported by the State Science Technology Program "Nanotechnology and nanomaterials" Project No 6.22.1.9.

REFERENCES

1. K. Hara, T. Horiguchi, T. Kinoshita, et al., *Sol. Energ. Mater. Sol. C.* **64**, 115 (2000).
2. A.M. Aegerter, *Sol. Energ. Mater. Sol. C* **68**, 401 (2001).
3. K. Tanabe, *Catal. Today* **78**, 65 (2003).
4. F. Dolci, M. Di Chio, M. Baricco, E. Giamello, *J. Mater. Sci.* **42**, 7180 (2007).
5. B. Zielinska, E. Borowiak-Palen, R.J. Kalenzuk, *J. Phys. Chem. Solids* **69**, 236 (2008).
6. P. Wilhelm, D. Stephan, *J. Photochem. Photobiol. A.* **185**, 19 (2007).
7. S. Khalameida, V. Sydorchuk, V. Zazhigalov, *Chem. Phys. Technol. Surf.* **2**, 253 (2011). [in Ukrainian].